



# Batteries and Electrochemical Capacitors

by Daniel A. Scherson and Attila Palencsár

The invention of the battery can be attributed to Alessandro Volta (1745-1827) of Como, Italy, who in 1800 described an assembly consisting of plates of two different metals, such as Zn and Cu, placed alternately in a stack-like fashion separated by paper soaked in an aqueous solution, such as brine or vinegar. As discovered by Volta, this contraption was capable of producing an electrical shock when its ends were touched. In a broad sense, batteries can be defined as devices that convert chemical into electrical energy using electrodes, immersed in media (liquids, gels, and even solids) that support the transport of ions, or electrolyte. This mode of operation is fundamentally different from that associated with conventional solid-state capacitors, invented about half a century earlier in Leyden, The Netherlands, in which charge is physically stored in nonreactive electrodes separated by a dielectric, or insulating material. However, the latter shares important commonalities with yet another class of devices developed much later known as electrochemical capacitors, which, as described later in this article, rely on charge separation at electrode|electrolyte interfaces to store energy.

Automotive, communications, and a host of consumer market applications, introduced in the first quarter of the twentieth century, made batteries a household term. However, the technological explosion brought about by the advent of the transistor and the concomitant miniaturization of electronic circuitry (as eloquently evidenced by the seemingly ever-evolving multifunctional cell phones, portable digital assistants, laptop computers, digital cameras, games, and, more recently, portable media devices, such as the iPod), may be regarded as perhaps the major factor responsible for batteries becoming among the most ubiquitous devices ever invented. Further major market expansions are expected from the

impending introduction of large fleets of gasoline-electric hybrid vehicles, which will help alleviate, at least momentarily, the worldwide impact on the economy and the environment induced by the inexorable depletion of fossil fuels and the release of greenhouse gases into the atmosphere. Driven primarily by a fast-growing and highly competitive market and the support of governments, scientists and engineers in industry, academia, and national laboratories have engaged in a frenzied search of means for maximizing battery performance in terms of power and capacity, *i.e.*, the actual charge the device can store, while minimizing weight and volume and mitigating safety risks.

## General Considerations

Batteries consist of single (although the term defines a collection), or multiple galvanic cells, connected in series to generate higher voltages. For example, in a car battery, six individual 2.0 V lead-acid cells provide 12 V. Each such cell consists of two electrodes: the anode, or source of electrons, and the cathode, or sink of electrons, labeled, respectively, as negative and positive in consumer batteries. Whereas the voltage of a cell ( $E_{\text{cell}}$ ) is prescribed by the nature of the chemical reactions at the two electrodes, the power it can deliver, defined as the product of the voltage ( $E$ ) and the current ( $I$ ), are governed by much more subtle factors. Some batteries can be used only once, so-called non-rechargeable or primary, and others multiple times, rechargeable or secondary. The most common primary battery, *i.e.*, Zn|MnO<sub>2</sub>, is depicted in Fig. 1a. For this system, the anode is a collection of Zn metal particles dispersed in a strongly alkaline aqueous solution mixed with a polymer, and the cathode is a hollow molded cylinder made out of MnO<sub>2</sub>. Direct physical (electronic) contact between the two electrodes (and, thus,

(continued on next page)

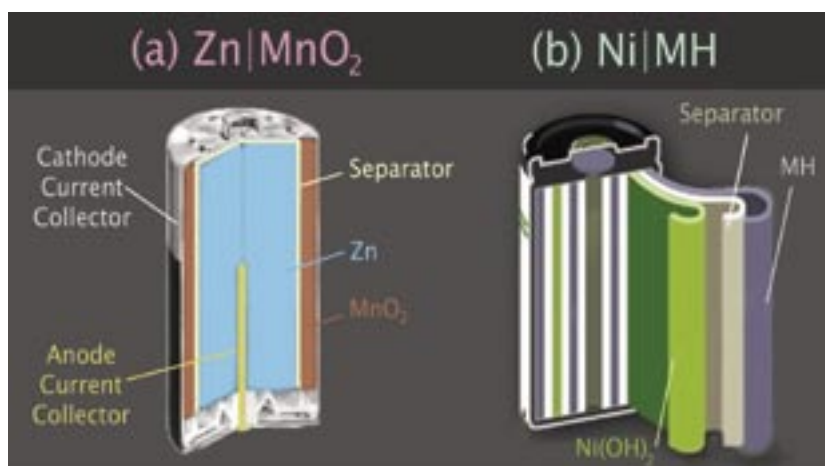


**Fig. 1.** (a) Schematic diagram of commercial primary (non-rechargeable) Zn|MnO<sub>2</sub> and (b) secondary (rechargeable) Ni|MH batteries. Adapted with permission from the manufacturers.

## Batteries and Electrochemical Capacitors

(continued from previous page)

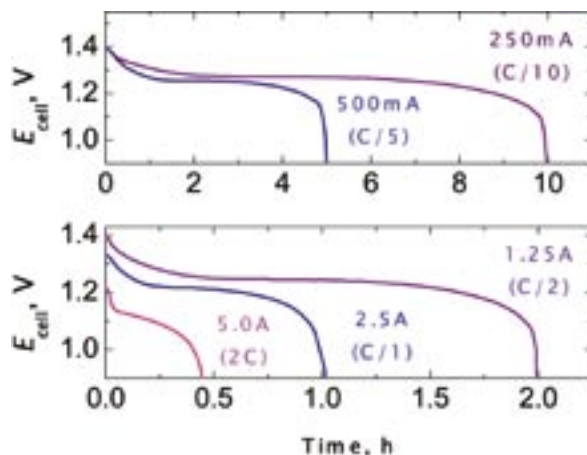


**Fig. 2.** Cell voltage ( $E_{\text{cell}}$ ) vs. time (in hours) for the discharge of a AA NiMH battery at various constant currents as indicated. Adapted with permission from the manufacturer.

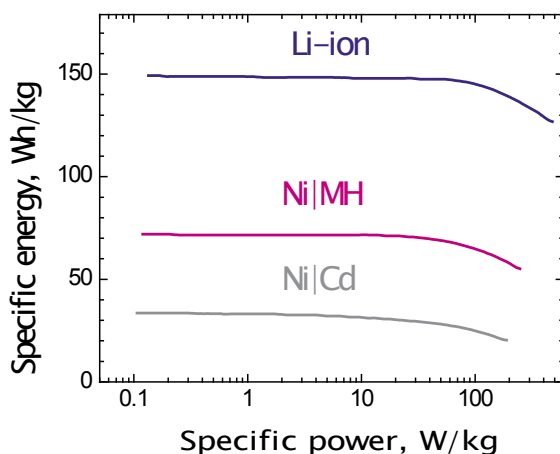


**Fig. 3.** Specific energy vs. specific power or Ragone plots, for three common rechargeable batteries. Ref: Handbook of batteries, D. Linden, T. B. Reddy, Eds., McGraw-Hill, New York (2002), 3rd Edition.

a short) is prevented by placing a non-woven fabric or separator between them, which also serves to hold sufficient electrolyte to establish ionic continuity within the battery. The intrinsic electronic conductivity of  $\text{MnO}_2$  is too low to sustain high currents; hence, a conductivity enhancer, most commonly a high surface area graphitic carbon, must be incorporated into the cathode to improve its performance and a polymeric binder for mechanical stability. Electrons are generated at the anode, via the oxidation of metallic Zn to yield a  $\text{Zn}^{2+}$  species, a two-electron transfer process, and are collected by a metal pin current collector inserted in the Zn paste as shown in Fig. 1. After flowing through the load, such as a light bulb, the electrons are delivered through a steel casing current collector, to the  $\text{MnO}_2$  cathode, where the  $\text{Mn}^{4+}$  ions are reduced to a lower valent state.

The voltage of an off-the-shelf Zn|MnO<sub>2</sub> cell, as measured with a high impedance voltmeter (which draws only a miniscule current) is  $E_{\text{cell}} \sim 1.5$  V. This value corresponds to the sum of the individual half-cell potentials of the two electrodes, as predicted by the corresponding Nernst equations, although the precise nature of the electrochemical reactions involved have been the subject of much heated debate. During operation,  $E_{\text{cell}}$  is always smaller than its open-circuit value (no load) and a function of both the demands imposed by the device it powers and the depth to which the battery has been discharged.

An example of a popular rechargeable system is the Ni metal hydride (Ni|MH) battery,  $E_{\text{cell}} \sim 1.2$  V, shown schematically in Fig. 1b. Its active cathode material is nickel hydroxide,  $\text{Ni}(\text{OH})_2$ , which has a layered-type crystal lattice, and the

anode, denoted as MH, consists of an alloy incorporating an array of mainly rare earth elements (or mischmetal). During charging, the metal sites in  $\text{Ni}(\text{OH})_2$  undergo oxidation to yield  $\text{NiOOH}$ , whereas the anode reduces water to elemental hydrogen, which combines with the metal to form a hydride, a virtual hydrogen storage. The construction of this battery differs from that of Zn|MnO<sub>2</sub> in that the electrodes are sandwiched with the separator in between and wound to form a cylinder, resembling a jellyroll.

Selection of a battery for a specific device is often made based primarily on its performance characteristics. One such figure of merit is obtained by applying a constant current ( $I$ ), while monitoring  $E_{\text{cell}}$  as a function of time. Shown in Fig. 2 is a plot of  $E_{\text{cell}}$  vs. time for various  $I$  for an AA Ni|MH battery. As indicated therein, for  $I = 250$  mA (see purple curve, top),  $E_{\text{cell}}$  decreases slowly during the first 2 h to reach a fairly constant plateau. After about 6 h,  $E_{\text{cell}}$  once again drops first slowly and then suddenly at about 10 h signaling the end of the battery useful life. Based on the observed lifetime, the charge or capacity the battery can deliver under these conditions, is  $10 \text{ h} \times 3600 \text{ s/h} \times 0.25 \text{ A} = 9000$  coulombs (denoted C), or in battery technology units, 2500 mAh ( $250 \text{ mA} \times 10 \text{ h}$ ). If  $I$  is increased, for example, to meet the demands of a more power hungry device, the observed useful life of the battery is obviously shorter, as illustrated by the blue curve, Fig. 2 top, for  $I = 500$  mA. Nevertheless, based on the same calculation presented above, the useful capacity of the battery remains virtually unchanged. Manufacturers often quote discharge rates in units of C (which, although it bears the same symbol, is not to be confused with that for coulombs) where C/1 corresponds to the current at which the useful capacity of the battery is consumed in 1 h. For the results shown in Fig. 2 top, the capacity of the battery for  $I = 250$  and 500 mA was exhausted in 10 (purple curve) and 5 h (blue curve), which corresponds to discharge rates of 0.1 C (or C/10) and 0.2 C (or C/5), respectively.

As the C rate is increased beyond a certain limit, however, the capacity of the battery can no longer be fully utilized. This is clearly illustrated for the AA Ni|MH battery discharged at 2 C (see magenta curve, Fig. 2 bottom), for which the lifetime falls short of the 0.5 h predicted based on the results obtained at the lower C rates. A fraction of valuable electrode material remained unused, an effect found for all battery systems for sufficiently high C rates. It is a challenge faced by scientists and engineers to find means of avoiding this

undesirable and wasteful phenomenon. This task requires a deep understanding of the underlying processes involved, which are almost always linked to hindrances in the transport of charged species.

A useful means of representing the operational performance of batteries and other energy storage and energy conversion devices is a graph of specific energy ( $A \times V \times h/kg = W \times h/kg$ ) vs. specific power ( $W/kg$ ). This graph is known as a Ragone plot, and is shown in semilog form for three common rechargeable batteries including Ni|MH in Fig. 3, derived from measurements of the type shown in Fig. 2. It becomes evident from these data, that the Li-ion battery has twice the specific energy compared to Ni|MH, and four times that of Ni|Cd, a system expected to be gradually displaced by Ni|MH, and Li-ion, due to environmental impact concerns. Although specific energy and specific power are important, other factors must also be considered when selecting a battery system for a specific application, including reliability (critical for pacemakers), safety, self-discharge, temperature, and even humidity (key for Zn|air hearing aid battery). This latter device is a cross between a battery and a fuel cell, in that the reaction at the (gas permeable) cathode is the reduction of oxygen from the atmosphere.

From an overall perspective, Li-ion batteries, today's canonical power source for portable electronics, undoubtedly represent the most promising energy storage system for a host of other applications, including transportation; hence, certain aspects of its principles of operation deserve particular attention.

### Li-Ion Batteries

The discovery of transition metal oxides,  $LiMO_2$  (where  $M = Ni$  or  $Co$ ) as reversible lithium-ion cathodes displaying very positive operating potentials was made by J. Goodenough (then at Oxford, and currently at the University of Texas, Austin) in the 1970s. In particular,  $LiCoO_2$  proved a key to the development and commercialization of secondary Li-ion batteries by Sony Corp. (a non-traditional battery company) as power sources for many of their own electronic devices. A schematic representation of the elementary redox processes associated with the operation of the Li-ion battery is shown in Fig. 4. During charging, lithium ions,  $Li^+$ , are released from the  $LiCoO_2$  lattice to the electrolyte solution incorporating a suitable salt, such as  $LiPF_6$  in an organic (aprotic) solvent, commonly a mixture of alkyl carbonates. At the same time,  $Li^+$  ions are inserted into the layered graphite structure from the electrolyte solution. These reactions

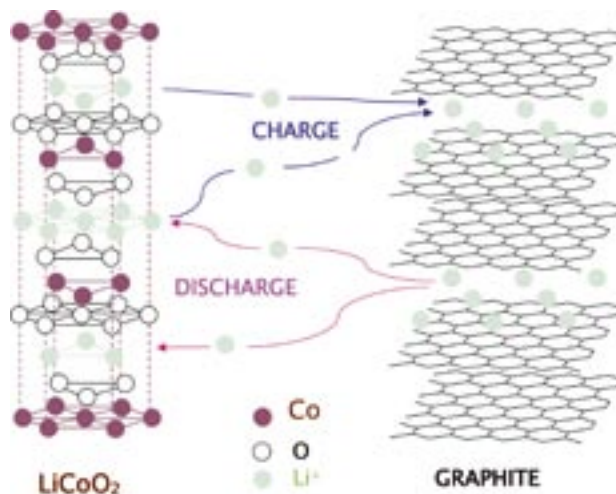


**Fig. 4.** Schematic diagram of the mode of operation of a  $LiCoO_2$ /graphite battery. During charge  $Li^+$  ions are released from  $LiCoO_2$  and injected into the graphite lattice. The reverse processes occur during discharge.

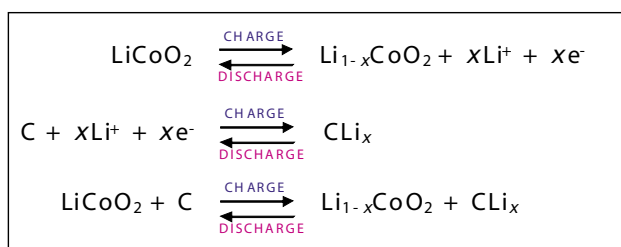


**Fig. 5.** Single electrode and net reactions for the  $LiCoO_2$ /graphite Li ion battery.

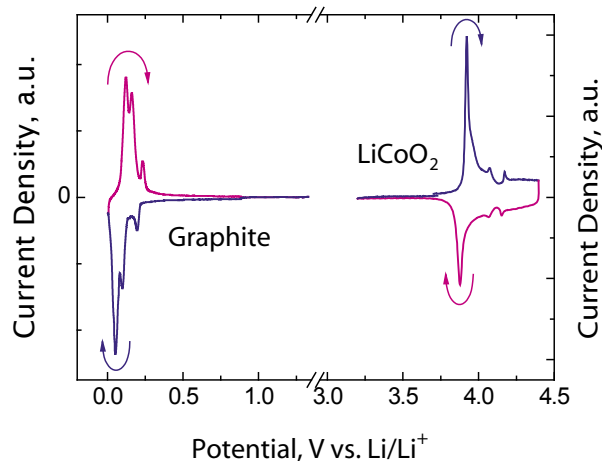


**Fig. 6.** Composite, semiquantitative (arbitrary current scale) cyclic voltammograms for natural graphite and  $LiMn_2O_4$  recorded independently at very slow scan rates. Data were obtained in a  $LiPF_6$  solution in a mixture of alkyl carbonates. The arrows indicate the direction of the potential scans and the blue and magenta represent charge and discharge, respectively. Refs: H. Wang and M. Yoshio, *Journal of Power Sources* 93, 123-129 (2001), and Dana A. Totir, Boris D. Cahan and Daniel A. Scherson, *Electrochimica Acta* 45, 161-166 (1999)

are reversed during battery discharge (see Fig. 5), which led to the coining of such terms as *rocking chair* or *shuttlecock* to describe more graphically its mode of operation. The actual electrodes are made of micrometer-size particles of graphite (anode) or  $LiCoO_2$  (cathode), mixed with relatively high surface area

carbon as a conductivity enhancer, as well as an organic binder to provide structural integrity.

A technique commonly used to gain insight into the properties of electrode materials, involves scanning

(continued on next page)

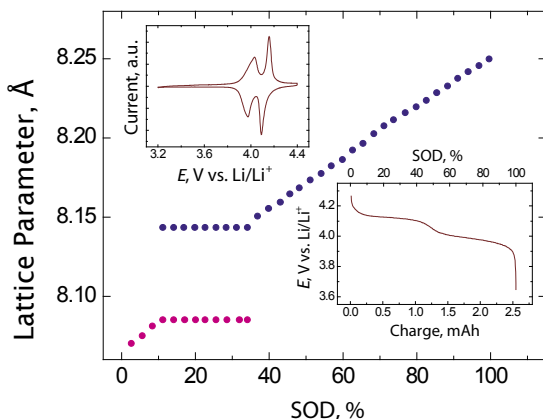


**Fig. 7.** Lattice parameter extracted from X-ray diffraction measurements collected in situ vs. SOD (%) for  $\text{Li}_x\text{Mn}_2\text{O}_4$  in the range  $0$  (fully charged)  $\leq x \leq 1$  (fully discharged). The presence of two distinct phases are represented by the blue and magenta circles. Top inset: Cyclic voltammetry of  $\text{LiMn}_2\text{O}_4$  in the potential region in which the redox transitions occur. Bottom inset: Potential (V vs.  $\text{Li/Li}^+$ ) vs. Charge (mAh) during the C/10 discharge of the electrode. Refs: T. Eriksson, A-K. Hjelm, G. Lindbergh and T. Gustafsson, *Journal of The Electrochemical Society*, 149 (9) A1164-A1170 (2002) and Dana A. Totir, Boris D. Cahan and Daniel A. Scherson, *Electrochimica Acta* 45, 161-166 (1999).

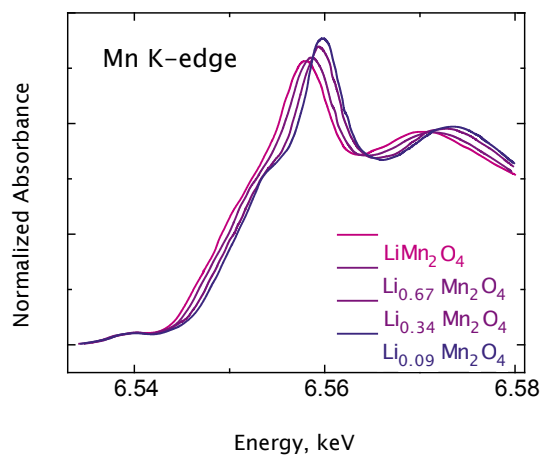


**Fig. 8.** Series of in situ Mn K-edge X-ray absorption spectra (normalized absorbance vs. energy in keV) for  $\text{Li}_x\text{Mn}_2\text{O}_4$  for  $x$  values specified. Ref: Youhei Shiraishi, Izumi Nakai, Toshio Tsubata, Takuhiro Himeda and Fumishige Nishikawa, *Journal Of Solid State Chemistry*, 133, 587- 590 (1997).

counterbalanced by the migration of  $\text{Li}^+$  in and out of the corresponding lattices. It thus follows from these data, and also confirmed experimentally, that the operating potential of the  $\text{LiCoO}_2$ /graphite battery is close to the separation between the peaks associated with reactions at the cathode and the anode, ca. 3.7 and 0.1 V vs.  $\text{Li}^+/\text{Li}$ , respectively. Furthermore, that the peaks found in the scans in the positive and negative directions are nearly mirror images is indicative that the reactions are energetically reversible, i.e., about the same potential difference, in principle, nominally required to recharge the battery.

Despite their extraordinary sensitivity, electrochemical measurements do not provide insight into the structural and electronic changes associated with the redox processes involved, for example, those responsible for the multiplicity of peaks found in the voltammetry in Fig. 6. Hence, other techniques must be used to gain access to such information. A better understanding of these factors may be regarded as critical to the rational design of materials displaying optimum performance characteristics. One approach involves a systematic structural and spectroscopic study of a group of lithium intercalation materials prepared individually spanning the entire range of Li content of relevance to the electrode operation, e.g.,  $0 \leq x \leq 1$ , for  $\text{Li}_x\text{CoO}_2$ , where  $x = 0$  and 1 corresponds to fully charged and fully discharged forms, respectively. Serendipitously, this laborious endeavor can be avoided by combining electrochemistry, as an expedient and highly accurate synthetic tool to prepare such group of materials, with X-ray based techniques, such as X-ray diffraction (XRD) or X-ray absorption spectroscopy (XAS) as structural and electronic probes. Furthermore, advantage can be taken of the high transparency to X-rays of carbon and other low-Z elements present in the main electrode constituents to perform such measurements *in situ*. For such experiments, charge is injected into the electrodes in small increments and the system allowed to reach equilibrium before data are acquired. Once completed, an additional charge is injected, and the whole procedure repeated until the desired  $\text{Li}^+$  range is covered. Alternatively, and depending on the time required for XRD or XAS data acquisition, charge can be injected at a constant and small enough (low C) rate for the system to maintain quasi-equilibrium conditions, while monitoring the potential and recording the desired data. These principles were fully exploited for studies involving the cubic spinel  $\text{LiMn}_2\text{O}_4$ , a “green” cathode material that

the potential of a single electrode (half-cell) in a linear fashion between two prescribed limits first in one direction and then in reverse, while monitoring the current, known as cyclic voltammetry. This method can be implemented with relative ease and provides an expedient means of screening new materials, as it requires very small quantities, even down to a single microparticle. Shown in Fig. 6 are cyclic voltammograms of natural graphite and  $\text{LiCoO}_2$  recorded independently in a solution of  $\text{LiPF}_6$  in a mixture of alkyl carbonates. The current axes in these plots are normalized for didactic purposes and the arrows indicate

the direction of the potential scan, where blue and magenta represent charge and discharge, respectively. These data were acquired at very low scan rates, on the order of a few tens of microvolts per second, to offset the sluggish diffusion of  $\text{Li}^+$  through solid lattices, which are orders of magnitude smaller than those of ions in liquid solutions, and allow for quasi-equilibrium conditions to be achieved over the entire potential range explored.

The clearly defined voltammetric features are ascribed to changes in the oxidation state of species within the electrode materials, which are



displays two well-defined voltammetric peaks at about 4.0 V vs. Li/Li<sup>+</sup> (top inset, Fig. 7). Analysis of a series of X-ray diffractograms for the (111) peak of LiMn<sub>2</sub>O<sub>4</sub> collected *in situ* during the C/10 discharge of the fully charged ( $\lambda$ -MnO<sub>2</sub>) cathode (bottom inset, Fig. 7), yielded, as shown in Fig. 7, evidence for the presence of one single phase (blue circles) for states of discharge (SOD), defined as the percent of the total capacity consumed, higher than 35%, and another single phase (magenta circles) for SOD < 10%, for which the lattice parameter varied linearly with SOD. As indicated in the figure, these two phases coexist for 10 < SOD < 35%.

Information regarding the oxidation state of the Mn sites as a function of SOD can be obtained from *in situ* XAS spectra, a technique in which the energy of the radiation is scanned over the range embracing the excitation of core, e.g., 1s, electrons to higher lying levels, including photoionization, or K-edge. Shown in Fig. 8 are a series of Mn K-edge XAS spectra in the form of normalized absorbance vs. energy (keV) for Li<sub>x</sub>Mn<sub>2</sub>O<sub>4</sub> for  $x$  in the range 0 ≤  $x$  ≤ 1 recorded *in situ* in a specially designed spectroelectrochemical cell. As the electronic density of the metal decreases, by virtue of an increase in the oxidation state, the nucleus becomes more effective in attracting the remaining electrons, making it more difficult for electrons in the same orbital to be removed. Hence, as the experimental data shows, the charging of the material leads to a shift in the energy required to photoexcite the 1s electrons toward higher energies, providing evidence that the electrons involved have predominantly metal character.

### Electrochemical Capacitors

Batteries (and also fuel cells) rely on chemical reactions at the electrodes to generate electrical energy. The behavior of certain electrode-electrolyte interfaces, however, resembles that of a conventional capacitor in that charge transfer across the interface over a limited voltage range, up to *ca.* 3 V, is greatly impaired. Even though the potential should be thermodynamically sufficient to drive one or more electron transfer processes, the rates at which such reactions proceed are negligibly small rendering the interface as effectively charged. Exceedingly careful experiments performed by Grahame toward the middle of this past century laid the foundations of our current knowledge of electrified interfaces. Key to the success of his experiments was the use of Hg electrodes, for which the surface could be renewed thereby avoiding problems with impurities. According to theory, one plate of the capacitor is

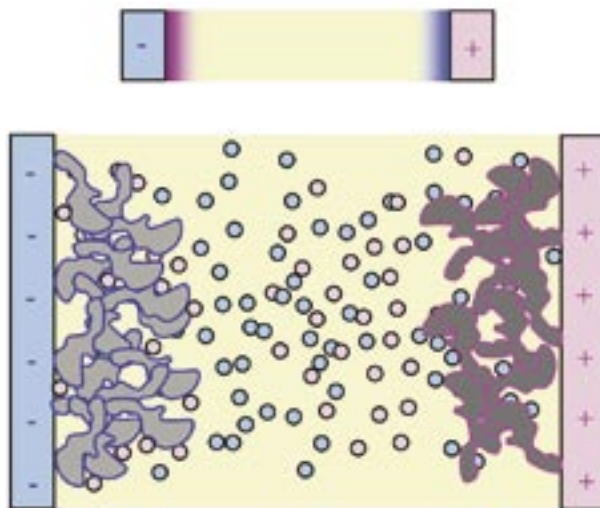


**Fig. 9.** (top) Schematic representation of a charged electrochemical capacitor and double layers at both electrode|electrolyte interfaces. Note that the device is two double layers in series, one at each electrode|electrolyte interface. Blue and magenta shades refer to net negative and positive charges. (bottom) Schematic representation of a charged high area carbon capacitor. The lines around the carbon (gray) particles represent either positive (magenta) or negative (blue) charges. Positive and negative ions (circles) are in pink and light blue, respectively.

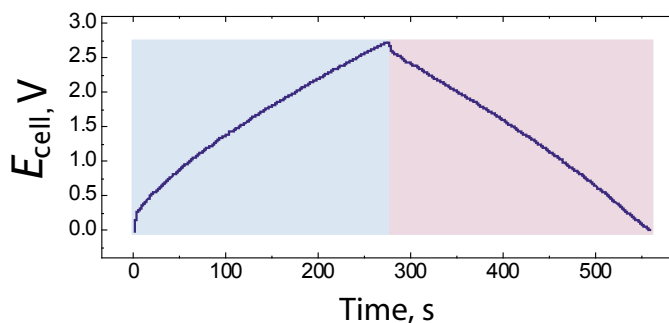


**Fig. 10.** Voltage profiles for the constant current charge (light blue) and discharge (pink) of a high area carbon electrochemical capacitor incorporating an organic solvent.

the electrode and the other is a collection of ions present in the electrolyte, forming a diffuse double layer of only a few nanometers thick (see Fig. 9 top for a schematic representation of a completely charged double layer capacitor). To preserve interfacial electroneutrality, the total charge of this diffuse layer must be equal and opposite to that which resides on the electrode. The actual specific double layer capacitance of solid electrode|aqueous solution interfaces,  $C_{dl}$ , is on the order of a few tens of  $\mu\text{F}/\text{cm}^2$ , and thus much higher than those found for conventional capacitors, and a function of the nature of both the electrode and the electrolyte solution.

Carbon is an unusual material in that forms displaying very high specific areas, up to 2000  $\text{m}^2/\text{g}$ , can be produced inexpensively. Assuming a  $C_{dl}$  of *ca.* 10  $\mu\text{F}/\text{cm}^2$ , a gram of such high-area carbon

should provide a capacity of 200 F, which could be matched only by a conventional capacitor of much larger dimensions. Advantage has been taken of this phenomenon to develop electrochemical capacitors based purely on carbon and suitable electrolytes with exceedingly high capacitances per unit weight or volume (see Fig. 9 bottom for a schematic representation of a charged carbon based capacitor). Note that the storage device is comprised of two (interfacial) capacitors connected in series. As a means of illustration, constant current charging (or discharging) of a high area carbon capacitor incorporating identical electrodes immersed in an organic electrolyte elicits a linear increase (or decrease) in the cell potential,  $E_{\text{cell}}$ , with time (see Fig. 10), as expected for a conventional capacitor. The very

(continued on next page)

## Batteries and Electrochemical Capacitors

(continued from previous page)

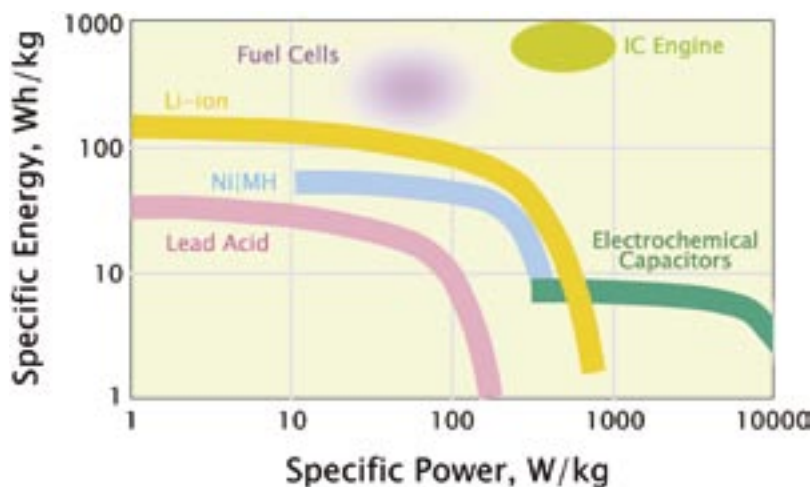


**Fig. 11.** Ragone plots for an array of energy storage and energy conversion devices. Ref: Venkat Srinivasan and John Newman: <http://berc.lbl.gov/venkat/Ragone-construction.pps>.

small vertical traces that are observed immediately following application or reversal of the current are due to voltage losses attributed to the internal resistance of the device or  $IR$  loss.

An appreciation of the advantage such an electrochemical capacitor, often referred to in the popular press as supercapacitor or ultracapacitor, offers compared to batteries can be gleaned from the Ragone plot. As shown in Fig. 11, electrochemical capacitors have superb specific power compared to batteries, but modest specific energies. This translates, in transportation terms, as good acceleration but poor range, which is precisely opposite to batteries or fuel cells, which are yet another type of electrochemical device in which the reactants are added to the electrodes to generate electricity (see contribution in this *Interface* issue from the Energy Technology Division). From practical and technological viewpoints, electrochemical capacitors are robust devices with excellent cycle life that can improve the effectiveness of battery-based systems by shrinking the volume of batteries required and reducing the frequency of their replacement.

Whether a battery, an electrochemical capacitor, a fuel cell, or a judicious combination of two or more of these, the level of sophistication involved in the design and manufacturing of a power source for a specific application, including microelectronics, transportation, and larger scale stationary stacks over the next few years may well approach the same degree of complexity as the devices they will power. A particularly intriguing prospect is the possibility of constructing three

dimensional batteries incorporating components of nanometric dimensions arranged in interpenetrating networks, to take advantage of short diffusional paths and thus higher currents than those achievable with present technologies. The advent of novel theoretical approaches and powerful computers is expected to deepen further our understanding of the factors that control both the energetics and transport dynamics of ions within well defined lattices. Such efforts are being complemented by ingenious tactics in combinatorial chemistry and simultaneous high-throughput screening of multiple electrodes that could well lead to the discovery of materials displaying unsuspected properties. ■

### Acknowledgments

The authors express their deep appreciation to N. Dudney, G. Blomgren, K. M. Abraham, B. Miller, R. Middaugh, R. Brodd, G. Amatucci, J. Miller, S. Sarangapani, and R. Corn for a critical reading of the manuscript.

### Suggested Readings

1. *Handbook of Batteries*, 3rd ed., D. Linden and T. B. Reddy, Editors, McGraw-Hill, New York (2002).
2. B. E. Conway, *Electrochemical Supercapacitors: Scientific Fundamentals and Technological Applications*, Kluwer Academic/Plenum Publishing, New York (1999).

### About the Authors

**DANIEL SCHERSON** is the Director of the Ernest B. Yeager Center for Electrochemical Sciences and the Charles F. Marbery Professor of Research in Chemistry at Case Western Reserve University. He is currently the chair of the ECS Battery Division

and an Associate Editor for the Journal of The Electrochemical Society. He may be reached at [Daniel.scherson@case.edu](mailto:Daniel.scherson@case.edu).

**ATTILA PALENCÁR** is a native of Romania and received his BS in chemistry at Babes-Bolyai University in Cluj Napoca, Romania. He is currently pursuing his PhD at Case Western Reserve University under the supervision of Daniel Scherson. He may be reached at [iap@case.edu](mailto:iap@case.edu).